Validation of a Health Monitoring In-Bed System using Speckle Patterns

Rafael S. Bento

***Abstract*— Ensuring the well-being of patients in medical facilities is the main objective of its medical staff, which includes not only treating the symptoms presented by patients, but also ensuring an efficient monitoring of their health status and preventing hazards caused by medical facilities related issues, such as bed falls or bed sores. Extensive bedding is the cause of such hazards, which can lead to extending the patient's stay in the medical facilities.**

The dissertation aims to validate a possible solution to the problem of bed sores by using optical fiber sensor-based technology. Such solution allows its prevention, through the continuous monitoring of patient's vital signs (breathing and pulsation) and movements, respecting the medical facilities privacy terms and maintain a low maintenance cost. The prototype aims to detect the disturbances made by the person's movements and vital signs, through the use of an optical sensor, on plastic optical fibers via speckle pattern analysis. In order to assess the efficiency of the sensor at identifying such disturbances, the shot transition detection methods of edge change ratio and correlation were used.

The data captured by the prototype was processed through the computation of the correlation and edge change ratio between consecutive speckle patterns. These computations made it possible to conclude that the optical fiber is sensible to 2 out of the 3 types of disturbances (movement and breathing), which can be used in the prevention of behaviors related to bed sores appearance.

***Index Terms*— Health Monitoring In-Bed (HMIB), Hospital Acquired Pressure Ulcers (HAPU), Plastic Optical Fibers (POF), Speckle Pattern, Vital Signs.**

I. Introduction

THE Health Monitoring In-Bed (HMIB) represents the medical staff monitoring of potential behaviors prone to cause accidents and medical problems, in order to guarantee the patient's overall health [1]. The higher work schedule originated by these accidents leads to a higher burden both in financial and human resources, thus making it necessary to implement efficient HMIB systems [2].

The type of accidents that show greater concerns among the HMIB field are the bed falls and HAPU (pressure ulcers created on the patient's body due to extensive bedding). It is estimated that among 0.295 % to 1.3 % of patients fall from their bed early and 67 % of the late bed falls detected lead to a premature death when compared to early detection falls [1]. The bedridden patients show a probability between 8 % and 40 % of developing HAPU due to a low ratio of Nurse-Per-Bed (NPB), turning HAPU detection into a serious concern [3], [4].

Although both of these problems represent a drain for the medical facilities resources, solutions for the bed falls problematic have proven to objectively improve the time period response rates in most medical environments [4]. On the other hand, it is harder to monitor HAPU because of the higher number of parameters needed to take into account and the difficulty in providing a good assessment [5], making the HAPU detection the main focus of the work.

A. State of the Art

Regarding the state-of-the-art in HAPU monitoring, one of the most universally accepted tool for the analysis of the risks that lead to HAPU is the Braden Scale [6]. Taking into account several parameters such as sensory perception, moisture, physical activity, mobility, nutrition and friction, the patient's caregiver attributes a number between 1 and 4 to each of those parameters when making the visual analysis. These numbers are given after corresponding guidelines of each parameter to the specific conditions of the patient, in order to obtain a final score.

There is an inverse relationship between the final score and the probability of the patient developing HAPU, making the Braden scale an effective tool to determine the risks of HAPU [6]. Its use isn't well prepared for a technological implementation, since there are parameters that can't be taken into account (nutrition and moisture) and are hard to objectively measure (activity and mobility). The lack of easy direct implementation of the Braden Scale in a technological implementation makes it necessary to use either some of its parameters or alternatives that experiment variations linked to the appearances of HAPU.

Regarding the necessary conditions and parameters for a working HAPU prevention system, the following characteristics are necessary: easy integration into the workload of the medical staff that doesn't contribute to a significant extra workload, since the ratio of NPB is currently too high [1], [7];

R. S. Bento is with the Department of Electrical and Computer Engineering, Instituto Superior Técnico, University of Lisbon, Lisbon, Portugal (e-mail: rafael.bento@ist.utl.pt).

non-interference from the environment characteristics of medical facilities on the performance of the HAPU system [7]; balance the use of the HAPU system with the periodic check-ups; low-cost resource requirement, since each medical facility must provide the detection for each one of the patients in need of it. The access of the state of the patient by using his vital signs can complement his movement's readings as signals to be used in an idealized HAPU prevention method.

With these characteristics in mind, the access of the state of the patient by using his vital signs can complement the information from his movement's readings as the type of disturbances to be used in the detection validity of the prototype.

B. Dissertation Objectives and Outline

The main objective of the dissertation is to develop and test a prototype system based on an optical sensor, by analyzing the speckle patterns emitted by optical fibers. The prototype is intended to be a confirmation of the viability of a scenario considered as a HAPU prevention system. The considered scenario will be presented in the "Proposed HAPU Prevention solution" section. After discussing the prototype developed for the detection of the disturbances, a series of tests will be made to assess them. In the final section, a discussion of the results and conclusion of the viability of the considered system is presented.

II. Theoretical Background

A. Fiber Optic Sensors

The use of fiber optic sensors is appropriate for a HAPU solution, due to the following characteristics: decreased weight and size that makes them less intrusive for medical environments; inexistence of sparks considered as a necessity in risk-free environments; low financial costs that lower the financial burden of the extra care required for a high number of patients [8].

Since there are a multitude of fiber optic sensors types to choose from, it is important to narrow it down to the most appropriate for the current application. The chosen type of fiber optic sensor that presents itself as the most suitable candidate in the prototype design is the Plastic Optical Fiber (POF), due to the following characteristics: high flexibility in bending and sensitive to strain, which means that it can withstand high amount of pressure; excellent combability with organic materials and capacity to not create shards when broken, which is beneficial in a risk-free environment; high resistance against damage and temperature variable environments, which guarantees the longevity of the system [9].

The signal travels inside the POF with the use of total internal reflection in its core. The points of contact between the individual light waves will result in either a constructive interference or in a deconstructive interference, which results in a light phenomenon dubbed as the granular spatial speckle pattern [10]. The speckle pattern serves as the method to analyze the influence that the disturbances chosen to be tested in the prototype have and conclude on the capability of detecting them.

B. Speckle Pattern

The speckle pattern is a phenomenon resulting from the interference between different angles of wavelets, resultant of the coherent signal originated by the POF, when they come into contact with one another. Fig. 1 shows a granular spatial speckle pattern obtained as an example of the intended output to be analyzed by the prototype used, where the black and white dots correspond to deconstructive and constructive interference, respectively [11].

Figure 1 – Example of a speckle pattern.

C. Vital Signs

The vital signs of breathing and pulsation are signals to be validated regarding the detection of the considered HAPU prevention system which, as in the case of a person's movements, will be made through the speckle pattern analysis. The breathing performed by a patient can be assessed with the acceleration of his chest, while the pulsation can be assessed by the mechanical activity performed by the cardiac muscles or with the heart sounds. Considering the situation of a patient lying down on a bed and with minimal activity, a range of $[10, 30]$ breathings per minute are considered for the majority of patients in these conditions ($[12, 18]$ for adults and $[10, 30]$ for adults over 80 years old), which corresponds to a frequency domain of $[0.17, 0.5]$ Hz. Regarding the pulsation readings, the range of normal pulsations per minute is considered to be $[45, 120]$, which corresponds to a frequency domain of $[0.75, 2]$ Hz [12].

In order to analyze the information provided by the changes in the speckle made from both types of disturbances, shot transition detection methods will be applied on the speckle patterns.

D. Detection of Changes in Speckle Pattern Images

In order to analyze the contents of a speckle pattern video and identify the timeframes where the disturbances occur, its content will be separated into multiple shots, in order to detect the sequence where transitions identify the moment of disturbances. The algorithms detecting shot transitions follow a common methodology: the scoring phase, where each set of frames f_i and f_{i+1} is compared between themselves, by

attributing a score to each one of them that is specific to the type of algorithm used. The difference between each set of frames gives the score to be considered in it [13]; the thresholding phase, where for the score of each set contained in a video, a threshold value is calculated, which serves the purpose of identifying if the score is high enough to be considered as a transition (positive hit). If the score doesn't cross the threshold, it is considered a false hit [13].

The two shot transition detection algorithms used in the work, represented in the scoring phase, are the correlation and Edge Change Ratio (ECR). Considering the coordinates x and y seen in the speckle pattern of the POF and the distribution levels of the intensity levels in the reference $p(I_1)$ and the disturbance $p(I_2)$, the correlation between the two can be given by

$$\mathbf{C} = \frac{\langle \mathbf{p(I_1)(x,y)p(I_2)(x,y)} \rangle - \langle \mathbf{p(I_1)(x,y)} \rangle \langle \mathbf{p(I_2)(x,y)} \rangle}{\sqrt{\left(\langle \mathbf{p(I_1)^2(x,y)} \rangle - \langle \mathbf{p(I_1)(x,y)^2} \rangle \right)^2 \times \left(\langle \mathbf{p(I_2)^2(x,y)} \rangle - \langle \mathbf{p(I_2)(x,y)^2} \rangle \right)^2}}, \quad (1)$$

where the higher the value of the correlation, the lower the changes are between each speckle pattern. The main advantage of this method is providing a reliable way to identify abrupt transitions [14], [15]. ECR compares the content between two consecutive frames through the use of processes such as edge detection (identification of probable outlines of the objects of the frames) and dilation (use of a structuring element to expand the shapes of the objects contained in the frames). By comparing edge transformed frames with dilated frames, it is possible to calculate the probability of the objects of the frame f_i being in frame f_{i+1}. The main advantage of this method is providing a reliable way to identify gradual transitions, while also showing average results at identifying abrupt transitions [13], [15].

Taking into account the high variance of the data obtained through the use of the ECR algorithm when applying the disturbances, a dynamic threshold method defined with the characteristics of the data obtained with the scoring phase will be used. The parameter value of the correct identification of the transitions was approximately 1 for all the tests made (considering an interval range of [0, 1]).

III. Proposed HAPU Prevention Solution

A. Scenario Considered

Considering the main objective of the work of developing a prototype that detects information about vital signs and movement changes, the speckle patterns will be obtained through the prototype developed in the laboratory of IT. The shot transition detection algorithms are applied on the speckle patterns obtained, through the use of the *MATLAB*® software, in order to obtain $1D$ data for posterior analysis. The detected information will be the basis of the validation for a considered scenario that offers a simple and non-intrusive HAPU prevention system, with the integration in medical facilities in mind. Fig. 2 shows a representation of the considered HAPU scenario in a medical environment.

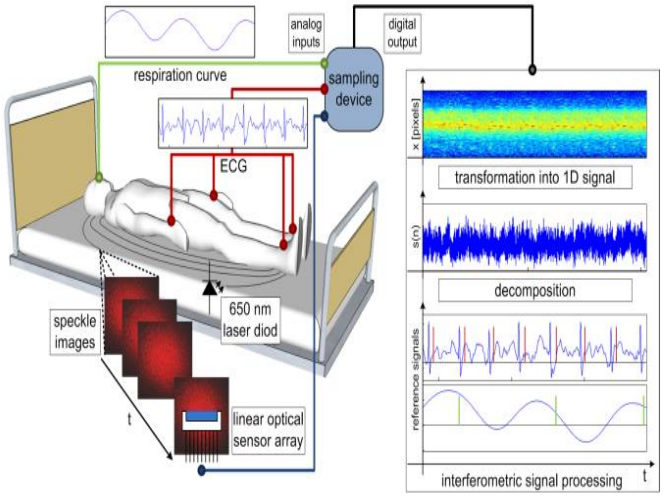

Figure 2 - Representation of the considered HAPU scenario in a medical environment [22].

The HAPU prevention system should have the POF directly in the surface where the patient rests, in order to identify both multiple speckle pattern images and changes due to the disturbances considered. The pulsation will present a more easily correlated speckle pattern due to its systematic nature, while the breathing can be more easily altered by the patient.

The speckle pattern images created by the vital signs and movement detected readings should be transformed into $1D$ data, in order to better analyze the disturbances. The decomposition of the data enables the correlation between the speckle patterns themselves and their corresponding signal's changes, by comparing pairs of video frames obtained from them.

B. Prototype Design

In order to detect the disturbances considered in the speckle pattern images, a prototype is needed to create visible speckles in the POF and posteriorly capture them. The hardware responsible for the speckle pattern capture will be a Raspberry Pi (RPI)1 (B model), while the processing of the video itself will be done through the *MATLAB@* 2017a version, since the low processing capacity of the RPI itself makes *MATLAB@* a good software choice. Regarding the architecture of the system used for video capture to be posteriorly processed by *MATLAB*®, fig. 3 shows its corresponding schematic.

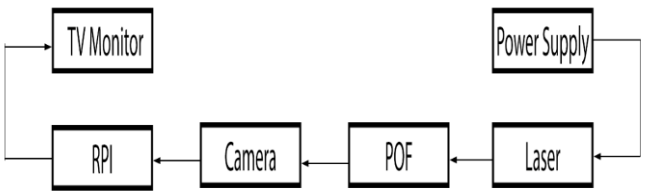

Figure 3 – Schematic of the video capturing setup.

An appropriate power supply powers the chosen laser through which its light will make visible the speckle patterns in the POF. The disturbances are applied during the signal acquisition period performed by the RPI, a process which is accompanied in real time through the connection of the RPI to a TV monitor. In order to exemplify the prototype signal acquisition, its corresponding schematic is shown in fig. 4.

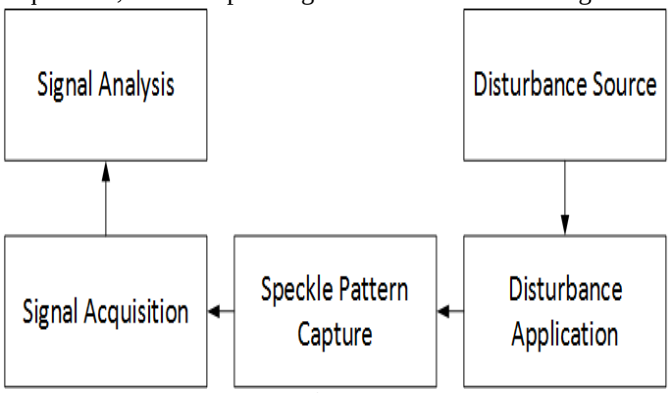

Figure 4 – Schematic of the prototype signal acquisition.

The acquisition of the speckle pattern images will be done through a setup mounted on the laboratory of Instituto de Telecomunicações to be show posteriorly. The visual information sent to the POF generates the speckle patterns themselves. The speckle patterns will be exported to *MATLAB®*, where they will be processed through the algorithms of correlation and ECR in order to validate the detection of the 3 types of disturbances.

The power supply, connected to the semiconductor laser, provides enough energy to perform the injection of a signal on the POF (5 volts). The laser used for the setup represented in fig. 5 is a CW532-001, which is manufactured by Roithner LaserTechnik [23].

The use of the RPI camera is a good choice in the context of capturing speckle patterns, since it enables a high sensibility of the video itself for detecting alterations in the speckle pattern, while also featuring low values of crosstalk and noise for obtaining videos with good quality. The RPI camera enables two types of Frames-Per-Second (FPS) configuration: 30 FPS for images with $1080p$ ($1920\ x\ 1080$ pixels) and 60 FPS for images with $720p$ ($1280\ x\ 720$ pixels) [24]. Since a higher quality of the images is more desirable than higher count of pixels for the speckle pattern analysis, the configuration used for the videos is the 30 FPS.

The POF used for the prototype, which has around $7\ m$ in length, is an HFBR-RUS100Z that is covered by a black thick of polyethylene and fabricated by Agilent Technologies [25].

The *RPI* used in the prototype has been chosen mainly for the video processing capabilities. The fact that it can easily have a camera attached to it also facilitates in the video capturing process [26]. The power source for this device must be around $3\ V$ with the use of a micro USB and an VMA404 transformer, with a current between the interval of $[0, 150]\ mA$ [25], [27].

In order to obtain images with the quality illustrated in fig. 1, it is necessary to adjust the parameters of the RPI camera, through the use of the raspivid command. The contrast parameter allows the adjustment of the speckle pattern perceptiveness, enabling a linear correlation between the contrast parameter and the readability of the speckle pattern itself. Considering its interval parameter of [0, 100], the chosen contrast value is 100.

The sharpness and the brightness parameter enable a better readability of the speckle pattern by increasing the quality of the speckle pattern dots and the light that affects them, respectively. Considering the interval parameter of [0, 100] for both parameters, the chosen value for the brightness and the sharpness are 100 and 20, respectively.

The saturation parameter presents an inverse correlation between its value and the number of border points available on the speckle pattern. In order to prevent the occurrence of this phenomenon, the saturation parameter should have a low value such as -80, considering an interval parameter of $[-100, 100]$.

The velocity parameter is responsible for the recording time period of the video and has an inverse correlation with the saturation of the image, while also showing a linear correlation with the sensibility to disturbances applied on the POF. The chosen mode for the RPI camera must then be the one with the higher exposition time, which corresponds to the "night time" mode.

The AWB parameter has a linear correlation with the luminosity of the images, making it difficult to assess the variations of the speckle pattern with high values of the AWB parameter. The chosen mode for AWB must then be the one with a lower value, which corresponds to the "sun" mode.

The video compression format used for the video capture is the h.264 for the 30-second videos and the h.261 for the 1-minute videos, due to the necessary lower bitrate for the higher recording time. The nearly lossless coding characteristic of this format makes it ideal to process the information from the speckle pattern. The application of a Region of Interest (ROI) in the obtained images is important to ensure that only the speckle pattern is analyzed. The ROI captures a smaller area of the images in order to be analyzed, with the respective coordinates of x, y, width and length being such that only the speckle pattern is analyzed.

The use of these configurations, in conjunction with the equipment previously described, makes it possible to design a prototype to assess the viability of the signals detection, shown in fig. 5.

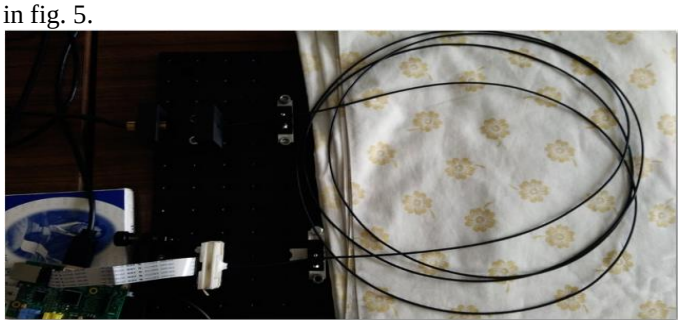

Figure 5 - Prototype setup for the video capture.

C. *Image Processing*

In order to reduce the amount of noise and interference in the videos captured, a lowpass equiripple filter is projected for all of the algorithms to be used. The filter was projected with the specifications of 1 KHz sampling frequency, 100 pass-band frequency, 150 stop-band frequency, 1 dB peak-to-peak ripple and 65 dB stopband attenuation. These specifications were chosen in order to maintain intact the overall 1D data output obtained from the algorithms implementation, while minimizing the noise characteristic present in them.

The chosen shot transition detection methods of correlation and ECR compare successive frames of a video, beginning at frame number 1 and ending at frame number N. Regarding the correlation method, the identification of lower values of correlation will indicate a higher degree of disturbances felt during the corresponding time-period of the set of 2 frames being compared. After the disturbances influence ends, the correlation values tend to a value closer to 1, representative of the stationary position of the POF. The derivative identifies the state of change in the correlation, where being positive corresponds to frames becoming closer in content and being negative corresponds to the frames growing apart in. Fig. 6 shows a flowchart representation of the successive correlation algorithm.

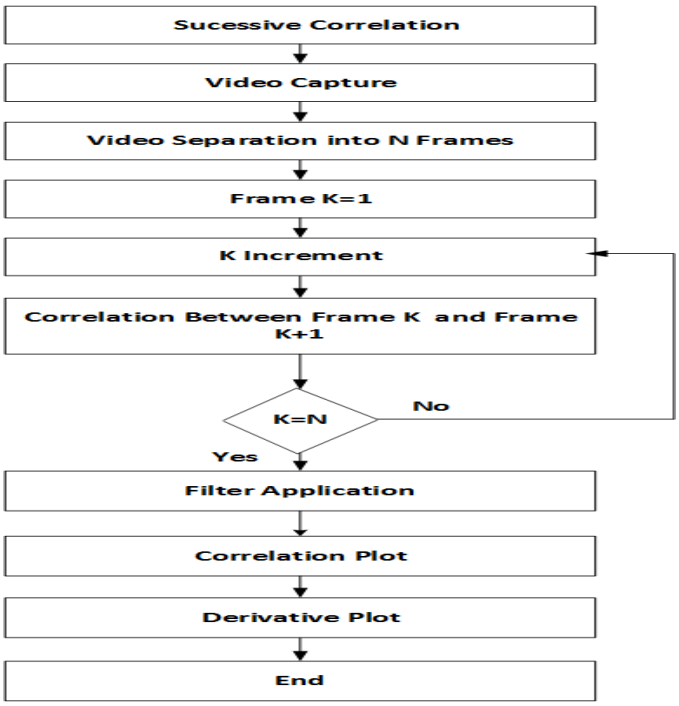

Figure 6 – Flowchart of the successive correlation algorithm.

Regarding the ECR algorithm, by computing the values for ECR in each iteration as $ECR = \max(\frac{ECR_n^{in}}{p_n}, \frac{ECR_{n-1}^{out}}{p_{n-1}})$, the increases in ECR can be used to identify the timeframes where a transition happens, when the value of ECR is greater than a specific threshold determined [18]. The corresponding nomenclature of the algorithm includes namely p_n (number of edge pixels in the edge detected frame n), p_{n-1} (number of edge pixels in the edge detected frame $n-1$), ECR_n^{in} (number of edge pixels in the frame originated by combining the dilated image of frame $n-1$ with the edge detected image of frame n) and ECR_{n-1}^{out} (number of edge pixels in the frame originated by combining the dilated image of frame n with the edge detected image of frame $n-1$). Fig. 7 shows a flowchart representation of ECR algorithm.

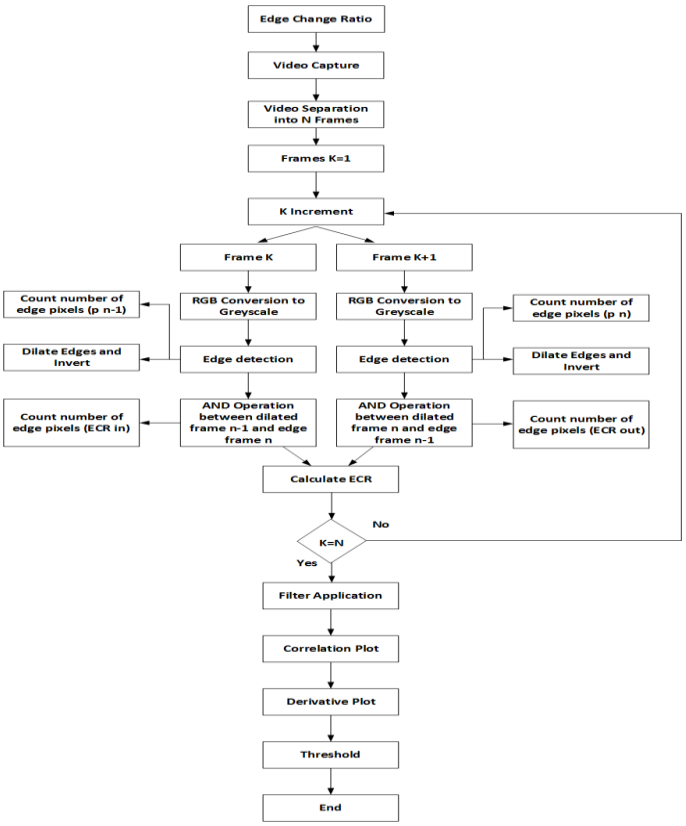

Figure 7 – Flowchart of the ECR algorithm.

The type of detector used for the process of edge detection is the canny edge detector. In addition to being a state of the art edge detector, it also has shown to be the one of the best when applied to speckle pattern frames [28]. Fig. 8 shows the application of 3 state of the art edge detectors applied to a video frame of one of the captured videoframes, which shows that the canny detector is indeed the best edge detector among the choices made.

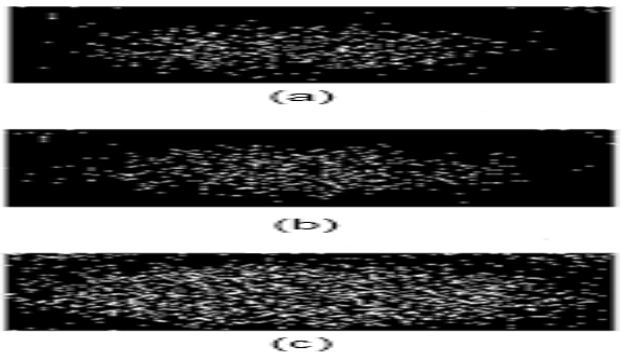

Figure 8 – Comparison between state of the art edge detectors. (a) Sobel; (n) Prewitt; (c) Canny.

IV. Experimental Evaluation

A. *Periodical Disturbance Assessment Tests*

The objective of the periodical disturbance tests is to assess the viability of frequency identification for the future assessment of breathing and pulsation. By placing a pendulum system over the aluminum breadboard and comparing its theoretical frequency of oscillation, obtained through counting its complete cycles, with the experimental frequency of oscillation, it will be possible to conclude about the reliability of identifying the oscillation frequency. Fig. 9 shows the pendulum placed over the aluminum breadboard.

Figure 9 – Pendulum placed on the aluminum breadboard.

In order to identify the frequency of oscillation, which presents the highest level of intensity, it is necessary to apply Fast Fourier Transform (FFT) to each of the tests made.

Considering the current tests for the pendulum, the corresponding frequency of oscillation, for an amplitude that is limited to small swings, can be approximated by counting the time period which takes the pendulum to complete a complete periodic movement and computing the corresponding frequency of the pendulum. Fig. 10 shows the pendulum test with a length used of $L \approx 6\,cm$, where the influence of a periodic movement with an expected frequency of $f_{pendulum} = 2{,}2\ Hz$ is analyzed. Since both the pendulum and the vital signs disturbances originate a considerably lower degree of change in the speckle pattern when compared to the movement disturbances, the application of the resultant adaptive threshold revealed to be ineffective for the ECR.

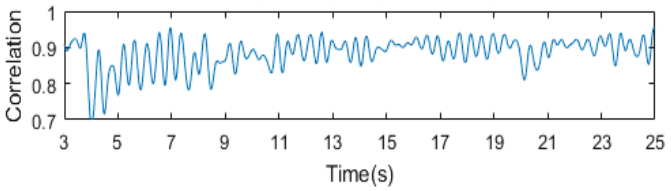

(a)

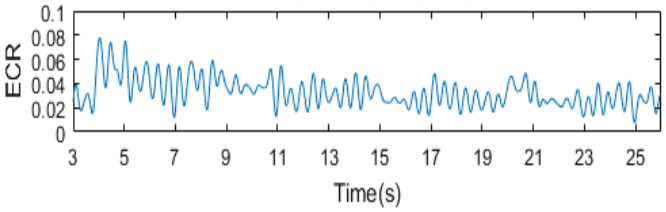

(b)

Figure 10 – Data for a pendulum with expected $f_{pendulum} = 2{,}2\ Hz$. (a) Correlation; (b) ECR.

Due to the lack of useful information taken from the derivative, those plots won't be shown up. The observation of fig. 10 shows the periodic movement of the pendulum beginning at $t = 3$ seconds and remaining in it throughout all of its duration. Since the expected value of frequency is $f_{pendulum} = 2{,}2\ Hz$, the range of frequencies used for the FFT is $[2, 3.5]\ Hz$. Fig. 11 shows the evolution of the single-sided amplitude spectrum of the data in a linear scale.

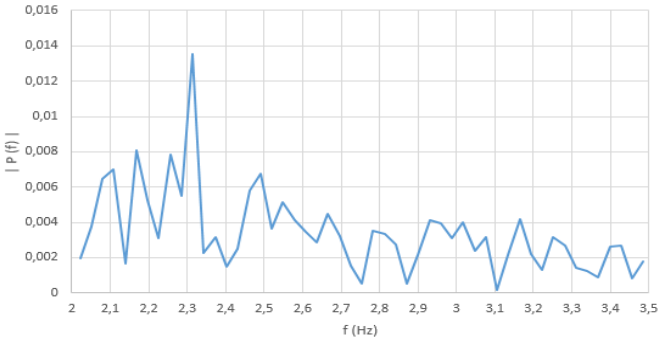

(a)

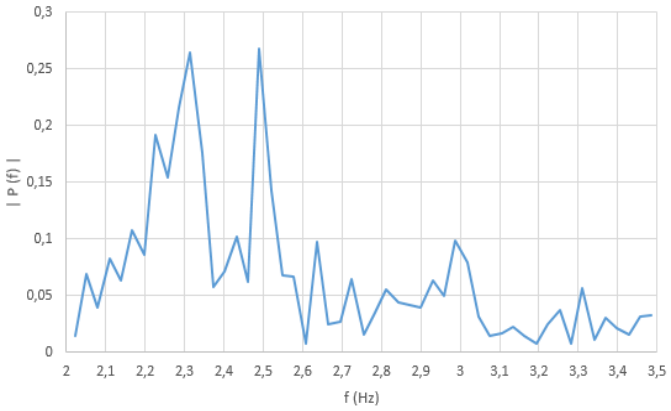

(b)

Figure 11 – Single-sided amplitude spectrum for a pendulum with expected $f_{pendulum} = 2{,}2\ Hz$ in linear scale. (a) Correlation; (b) ECR.

The observation of fig. 11 shows that a peak at $f \approx 2.3\ Hz$ was identified in the spectrums. Since the theorized frequency of oscillation is $f_{pendulum} = 2{,}2\ Hz$ and the pendular movement isn't perfect due to the format of the mass used, it can be concluded that its frequency of oscillation was successfully identified. The ECR data also identified the $f_{pendulum} = 2{,}5\ Hz$ which doesn't correspond to the true frequency of oscillation, therefore making the ECR algorithm

worse than the correlation algorithm at the frequency identification process.

With the detection of the frequencies with highest intensity level shown as viable for the prototype, the assessment tests made in the following section will correspond to the movement.

B. Movement Assessment Tests

Fig. 12 shows the movement test where the influence of a amplitude on a fixed disturbance is analyzed. The POF remains static until $t = 12$ seconds, upon which a $3\ cm$ fixed disturbance is applied.

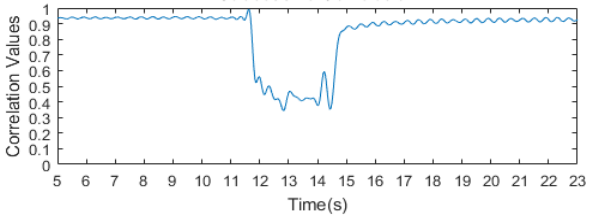

(a)

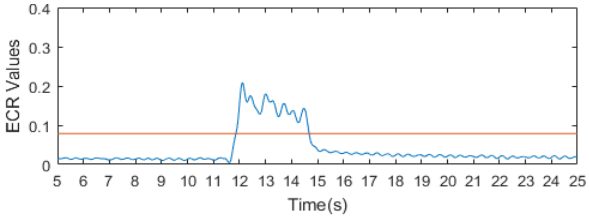

(b)

Figure 12 – Data for a 3 *cm* fixed disturbance. a) Successive correlation; b) ECR.

The observation of fig. 12 shows a clear identification of the disturbance in $t = 12$ seconds and of the moment where the POF is fixed at 1,5 *cm* in $t = 15$ seconds. In order to represent the quotient between the average values of the pre-disturbance and the disturbance time period, the graphs represented by fig. 13 were made. The quotient regarding the successive correlation data is represented by Δc, while the quotient regarding the ECR data is represented by Δe.

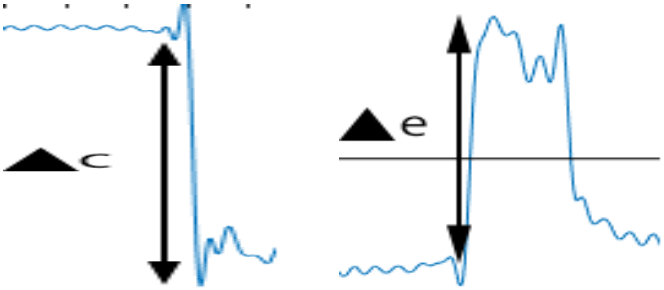

(a) *(b)*

Figure 13 – Representation of the quotients. (a) Δc; (b) Δe.

It is possible to represent the relation between the different amplitudes of the disturbances and the quotients represented in fig. 13. Fig. 14 represents this relationship for the data that is show not only in fig. 12, as well as different values of fixed amplitudes and orientation.

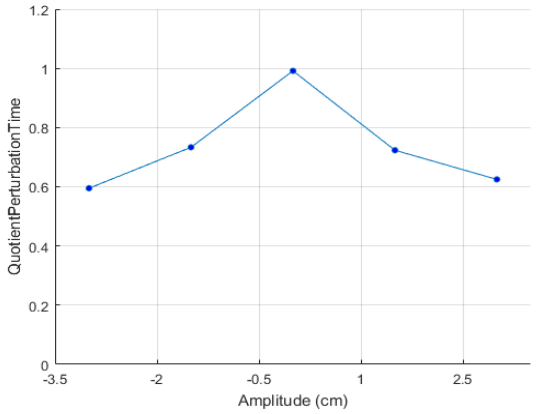

(a)

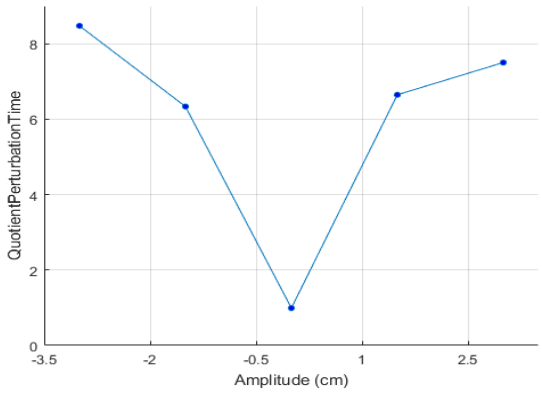

(b)

Figure 14 – Representation of the quotient between average values in the disturbance and pre-disturbance timeframe. (a) Successive correlation; (b) ECR.

The observation of fig. 14 (a) shows that the values of the quotients increase linearly with the decrease of the amplitude, with a value of $\Delta c \approx 1$ for a static POF. The observation of fig. 14 (b) shows that the values of the quotients decrease linearly with the decrease of the amplitude, with a value of $\Delta e \approx 1$ for a static POF. It can then be concluded that higher values of amplitude lead to higher variances of the quotient values.

Since there is no guarantee that the disturbances are isolated in the medical environment, it is important to evaluate the capacity of the prototype to detect successive disturbances. Fig. 15 shows the movement test where the influence of two fixed disturbances is analyzed. The POF remains static until $t = 10$ seconds and $t = 21$ seconds, upon which two $1{,}5\ cm$ fixed indirect disturbances are applied.

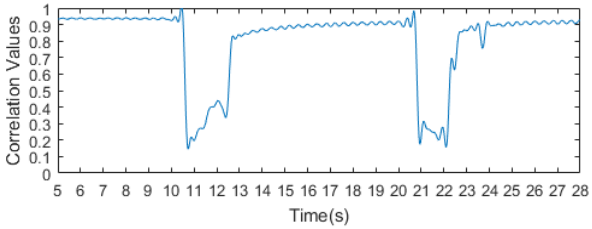

(a)

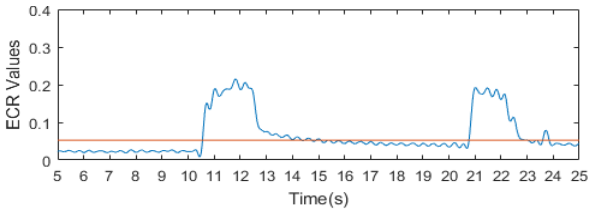

(b)

Figure 15 – Data for two 1,5 cm fixed disturbances. a) Successive correlation; b) ECR.

The observation of fig. 15 shows that the two disturbances can be clearly identified, as well as the first disturbance having no influence on the identification of the second disturbance. Fig. 15 (b) identifies the end of the second disturbance as being under its adaptive threshold value, which means that it isn't part of the hard cut. It can be concluded that both algorithms clearly identify successive movement disturbances.

Although only direct movement disturbances have been considered so far, it is important to analyze the influence of indirect disturbances applied on the aluminum breadboard. Fig. 16 shows the movement test where the influence of indirect disturbances is analyzed. Two groups of 5 indirect disturbances are applied at $t = 12$ seconds and $t = 22$ seconds, with a distance from the POF of 5 cm and 15 cm, respectively.

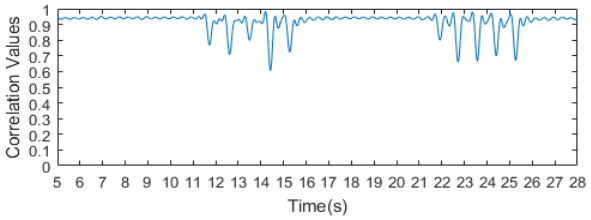

(a)

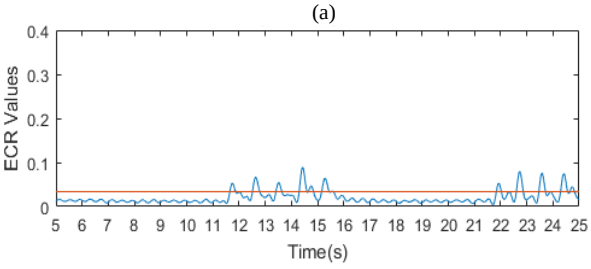

(b)

Figure 16 – Data for two sequences of indirect disturbances at 5 cm away from the POF. (a) Successive correlation; (b) ECR.

The observation of fig. 16 shows that, even with the static POF, the indirect disturbances can be clearly identified. The indirect disturbances were performed by dropping a box of approximately $200\,g$ on the surface from a height of approximately $10\,cm$, in order to roughly guarantee a similar force applied along the test. Since the results from the 5 cm and 15 cm tests show similar variations in their data, it can be concluded that the force applied from the falling object is the primary factor for the variations in the data.

Since both the successive correlation and ECR algorithms presented themselves as good methods for movement detection, they will be used in the future tests of the remaining disturbances.

C. *Breathing Assessment Tests*

The analysis of the breathing influence in the speckle pattern images is made through the identification of the frequency with the highest level of intensity in the spectrum. By placing a person on top of the aluminum breadboard as shown in fig. 5 while simultaneously performing breathing movements and staying still, the analysis of the breathing movements is done. The range of normal breathing frequencies for adults, which is represented by the interval of $[10, 30]$ breathings per minute, corresponds to the interval of $f = [0.17, 0.5]\,Hz$ for these types of tests.

For the breathing test made in order to assess results with an accelerated breathing rate of 20 breathings per minute, the corresponding frequency is approximately of $f_{breathing} = 0.33\,Hz$. Fig. 17 shows the breathing test where the influence of a breathing frequency of $f_{breathing} = 0.33\,Hz$ is analyzed.

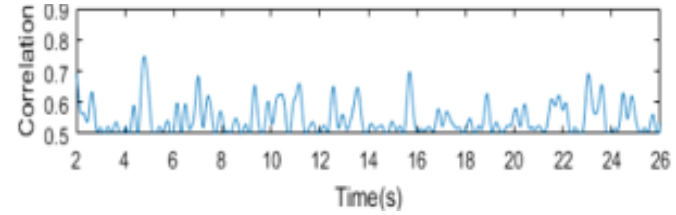

(a)

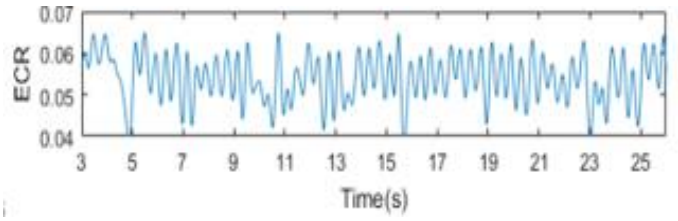

(b)

Figure 17 – Data for an expected breathing rate of $f_{breathing} = 0.33\,Hz$. (a) Correlation; (b) ECR.

The observation of fig. 17, in particular figure. 17 (a), shows the moments where the periodic breathing movements were performed, at $t \approx \{4, 7, 10, 13, 16, 19, 21, 23\}$. Since the expected value of frequency is $f_{breathing} = 0{,}33\,Hz$, the range of frequencies used for the FFT is $[0, 0.5]\,Hz$. Fig. 18 shows the evolution of the single-sided amplitude spectrum of the data in a linear scale.

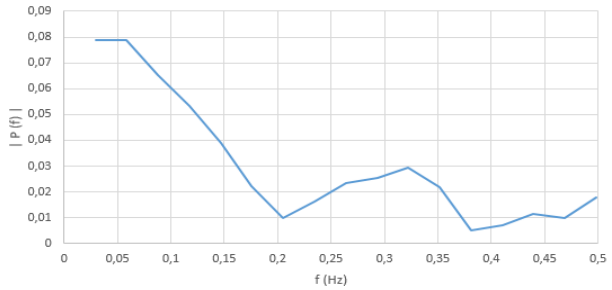

(a)

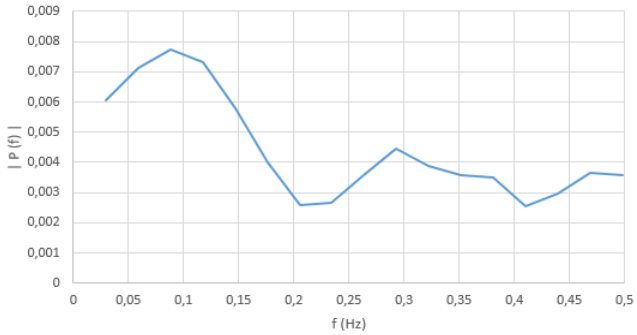

(b)

Figure 18 – Single-sided amplitude spectrum for a breath-rate of $f_{breathing} = 0.33\ Hz$ in linear scale. (a) Correlation; (b) ECR.

The observation of fig. 18 shows that the frequencies of $f_{breathing} \approx 0.32\ Hz$ and $f_{breathing} \approx 0.29\ Hz$ were identified in the amplitude spectrums, respectively, as well as an expectedly higher continuous component in the lower frequencies. The $f_{breathing} \approx 0.32\ Hz$ of the correlation data is closer to the expected $f_{breathing}$ when compared to the ECR data, which was expected both from the results previously obtained in the periodical disturbance assessment tests and in the current section.

D. Pulsation Assessment Tests

The analysis of the pulsation influence in the speckle pattern images is made through the identification of the frequency with the highest level of intensity in the spectrum. By placing the wrist of a person on top of the aluminum breadboard as shown in fig. 5, the analysis of the breathing movements is done. The range of normal pulsation frequencies for adults, which is represented by the interval of [45, 120] pulsations per minute, corresponds to the interval of $f = [0.75, 2]\ Hz$ for these types of tests.

The direct contact with the POF leads to the best result type when placing the wrist directly in contact with the POF. Fig. 19 shows the pulsation test where the influence of an expected pulsation frequency of $f_{pulsation} = 1.31\ Hz$ is analyzed, for a time period of 60 seconds.

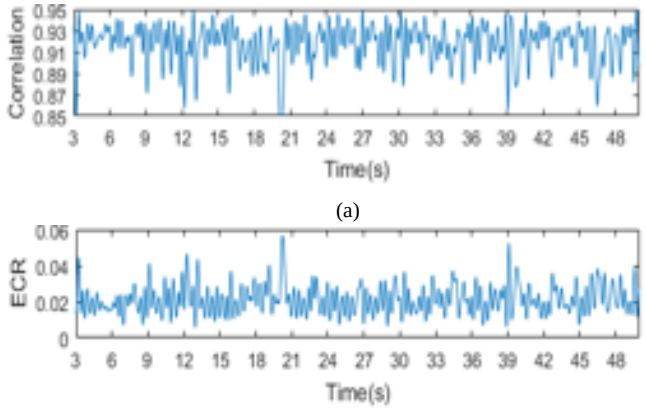

(a)

(b)

Figure 19 - Data for an expected pulsation rate of $f_{pulsation} = 1.31\ Hz$, in direct contact with the POF. (a) Correlation; (b) ECR.

Since the expected value of frequency is $f_{pulsation} = 1.31\ Hz$, the range of frequencies used for the FFT is $[0.75, 2]\ Hz$. Fig. 20 shows the evolution of the single-sided amplitude spectrum of the data in a linear scale.

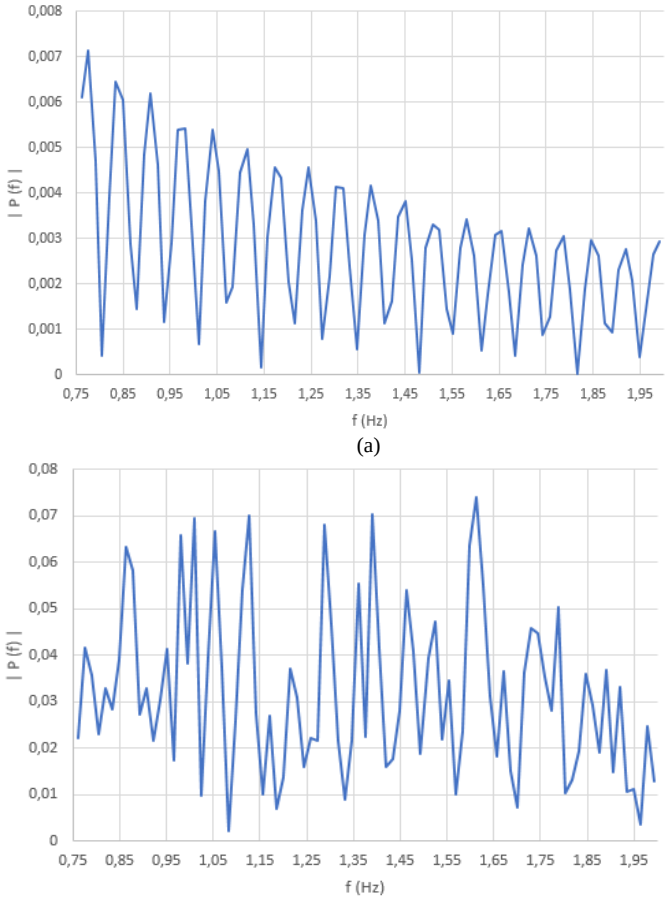

(a)

(b)

Figure 20 – Single-sided amplitude spectrum for an expected pulsation rate of $f_{pulsation} = 1.31\ Hz$ in linear scale, in direct contact with the POF. (a) Correlation; (b) ECR.

The observation of fig. 20 shows that the correlation data has no relevant information regarding the identification of the frequency of the pulsation. While fig. 20 (b) identifies $f = 1.6\ Hz$ as the experimental value for the frequency of pulsation, it strands too far away from the expected one to be considered a valid result. It can be concluded that the capability of detecting pulsation around the area of the POF is non-existent.

V. Conclusions

The analysis of the periodical disturbance assessment tests concluded that the FFT algorithm clearly identified the frequency of oscillation in the prototype, therefore proving its viability for the next disturbances assessment tests. The tests also showed that the correlation method provided a better identification of the frequency of oscillation when compared to the ECR method.

The analysis of the movement assessment tests concluded that both direct and indirect changes to the POF affect the speckle pattern. The tests also showed which shot transition

detection methods were ideal for the current application by providing a clear explanation of the advantages of the 2 methods accepted and a comparison between each type of movement disturbance. It was concluded that disturbances on the POF due to movements can be easily detectable.

The analysis of the breathing assessment tests concluded that their action leads to significant changes in the speckle pattern images and the FFT algorithm clearly identified the corresponding frequency of the data in the prototype. The tests also showed that, as previously demonstrated by the periodical disturbance assessment tests, the correlation method providing a better identification of the frequency of oscillation when compared to the ECR method. It was concluded that the disturbances on the POF due to breathing can be easily detectable.

The analysis of the pulsation assessment tests concluded both their action leading to a negligible difference in the data collected and the inability to clearly detect the pulsation itself through the FFT algorithm. The low intensity of the vital sign, compared to previous disturbances tested, corroborates the difficult identification of it. It was concluded that the disturbances on the POF due to pulsation can't be easily detectable.

The shot transition methods applied on the data taken from the prototype showed initial promise regarding the identification of the disturbances. Considering the entirety of the tests made and the corresponding advantages, the correlation method presents itself as the most appropriate for the intended application due to the better frequency identification and lower computational period-time.

In conclusion, the prototype provides the ability to detect both movement and breathing disturbances in a laboratory environment made to resemble the medical environment as shown in fig. 5.

References

[1] T. Gonnot, W. J. Yi, E. Monsef, P. Govindan and J. Saniie, "Sensor network for extended health monitoring of hospital patients," 2014 IEEE Healthcare Innovation Conference (HIC), Seattle, WA, 2014, pp. 236-238

[2] M. Heydarzadeh, M. Nourani and S. Ostadabbas, "In-bed posture classification using deep autoencoders," 2016 38th Annual International Conference of the IEEE Engineering in Medicine and Biology Society (EMBC), Orlando, FL, 2016, pp. 3839-3842.

[3] P. Kittipanya-Ngam, O. S. Guat and E. H. Lung, "Bed detection for monitoring system in hospital wards," 2012 Annual International Conference of the IEEE Engineering in Medicine and Biology Society, San Diego, CA, 2012, pp. 5887-5890.

[4] S. Ostadabbas, R. Yousefi, M. Faezipour, M. Nourani and M. Pompeo, "Pressure ulcer prevention: An efficient turning schedule for bedridden patients," 2011 IEEE/NIH Life Science Systems and Applications Workshop (LiSSA), Bethesda, MD, 2011, pp. 159-162.

[5] B. Braden and N. Bergstrom, "Clinical utility of the Braden Scale for predicting pressure sore risk.", Advances in Skin & Wound Care, vol. 2, no. 3, pp. 44-51, 1989.

[6] B. Braden and N. Bergstrom, "Clinical utility of the Braden Scale for predicting pressure sore risk.", *Advances in Skin & Wound Care*, vol. 2, no. 3, pp. 44-51, 1989.Langemo, Diane K. Et al "The lived experience of having a pressure ulcer: a qualitative analysis", Advances in Skin & Wound Care, vol. 13, no. 5, p. 225, 2000.

[7] P. W. Aung Aung *et al*, "Evaluation and analysis of multimodal sensors for developing in and around the bed patient monitoring system," 2010 Annual International Conference of the IEEE Engineering in Medicine and Biology, Buenos Aires, 2010, pp. 2159-2162.

[8] C. Mark, S. Brian, "Basics of Fiber Optics", in Amphenol Fiber Systems International, Allen, *TX*

[9] K. Peters, "Polymer fiber optic sensors - a review," Smart Mater. Struct. vol. 20, no. 1, pp. 013002-1–013002-17, 2011.

[10] Hägele, Clemens, et al "Plastic optical fiber curvature measuring technique based on Speckle Pattern image processing.", Universidade Federal do Espírito Santo, Goiabeiras Vitória, Brazil.

[11] W. Sharpe, Springer handbook of experimental solid mechanics, 1st ed. Baltimore, 2008.

[12] P. Podbreznik, D. Đonlagić, D. Lešnik, B. Cigale and D. Zazula, "Cost-efficient speckle interferometry with plastic optical fiber for unobtrusive monitoring of human vital signs", *Journal of Biomedical Optics*, vol. 18, no. 10, p. 107001, 2013.

[13] J. Bescos, G. Cisneros, J. Martinez, J. Menendez and J. Cabrera, "A unified model for techniques on video-shot transition detection", IEEE Transactions on Multimedia, vol. 7, no. 2, pp. *293-307, 2005.*

[14] Rodríguez Cobo, Luis, et al "POF vibration sensor based on Speckle Pattern changes." SPIE Society of Photo-Optical Instrumentation Engineers, 2012.

[15] R.LIENHART, "Reliable Transition Detection in Videos: A Survey and Practitioner's Guide", International Journal of Image and Graphics, vol. 01, no. 03, pp. 469-486, 2001.

[16] P. Podbreznik, D. Đonlagić, D. Lešnik, B. Cigale and D. Zazula, "Cost-efficient speckle interferometry with plastic optical fiber for unobtrusive monitoring of human vital signs", *Journal of Biomedical Optics*, vol. 18, no. 10, p. 107001, 2013.

[18] R.LIENHART, "Reliable Transition Detection in Videos: A Survey and Practitioner's Guide", International Journal of Image and Graphics, vol. 01, no. 03, pp. 469-486, 2001.

[19] P. Podbreznik, D. Đonlagić, D. Lešnik, B. Cigale and D. Zazula, "Cost-efficient speckle interferometry with plastic optical fiber for unobtrusive monitoring of human vital signs", *Journal of Biomedical Optics*, vol. 18, no. 10, p. 107001, 2013.

[20] J. Zubia and J. Arrue, "Plastic Optical Fibers: An Introduction to Their Technological Processes and Applications", *Optical Fiber Technology*, vol. 7, no. 2, pp. 101-140, 2001.

[21] O. Ziemann et al, *POF--polymer optical fibers for data communication.*, 1st ed. Springer Science & Business Media, 2013.

[22] P. Podbreznik, D. Đonlagić, D. Lešnik, B. Cigale and D. Zazula, "Cost-efficient speckle interferometry with plastic optical fiber for unobtrusive monitoring of human vital signs", *Journal of Biomedical Optics*, vol. 18, no. 10, p. 107001, 2013.

[23] Rodríguez Cobo, Luis, et al "POF vibration sensor based on speckle pattern changes." SPIE Society of Photo-Optical Instrumentation Engineers, 2012.

[24] Raspberry Pi Foundation [Online]. Available: https://www.raspberrypi.org/ [Acessed: 31-Nov-2017].

[25] Roithner Lasertechnik [Online]. Available: http://www.roithner-laser.com/laser_modules_dot_532.html [Acessed: 27-Dec-2017].

[26] Rs-Components, "Raspberry Pi Model B", *Prod. Data*, 2013.

[27] Raspberry Pi Foundation [Online]. Available: https://www.raspberrypi.org/ [Acessed: 31-Nov-2017].

[28] P. Kaur and R. Maini, "Performance Evaluation of Various Thresholding Methods using Canny Edge Detector", *International Journal of Computer Applications*, vol. 71, no. 9, pp. 26-32, 2013.

Rafael S. Bento was born in Setúbal, Portugal, on 27 January 1993. It is currently completing the Master in Electrical and Computer Engineering, specialization in Telecommunications and Computer at *Instituto Superior Técnico*, in Lisbon.